

Coulomb K_a , K_p Static and Dynamic for Clay

By Farid A. Chouery¹, P.E., S.E.

©2006 Farid Chouery all rights reserved

Abstract

This paper addresses the static and dynamic active and passive pressure for cohesive soil on a slanted wall with a sloped backfill. The solution is based on Coulomb method of extremum value of the earth pressure. In the static case, the active solution is compared with the Rankine method. The results show that the Rankine solution is **not** conservative and it is considered an approximation. The passive solution is compared with the logarithmic-spiral method of slices. The results show the cut-off value for positive wall friction to be less than $\phi/3$. Thus, the solution is not recommended to be used beyond the cut-off point. For the dynamic case, the solution is successfully compared with the free-field method using the corresponding wall friction and adhesion of the free field. Noting that the wall friction and adhesion of the free-field is specific and not as general as the proposed solution. The results show the free-field equations are slightly more conservative. The solutions are consistent with the classical methods and complete the Coulomb equations of earth pressures.

Introduction

There are cases where retaining walls are backfilled with cohesive material. It is known that the design of retaining structures for cohesive mass has much uncertain basis (see Kézdi in Winterkorn and Hsai-Yang (1975)[22]). For example the magnitude of

¹ Structural, Electrical and Foundation Engineer, FAC Systems Inc., 6738 19th Ave. NW, Seattle, WA

displacement required to produce a limit state of equilibrium cannot be determined equivocally. Thus, creep phenomena will occur that may vary the earth pressure. The extremum value of the earth pressure can only be taken into consideration for the dimensioning of the wall, if the creep movement is to occur without damage to the structure. Additionally, the extremum method requires the soil to be normally consolidated. While considering abandoning the use of cohesive backfill due to all these uncertainties, in many cases a cohesive backfill is unavoidable. For example: In the case of a shoring wall, where soldier piles are installed adjacent to the property line, the adjacent soil is cohesive. In this case and many others it requires the active and passive earth pressures for cohesive material. Prior work in static has been done by Prabhakara (1965)[12]. He gave the active pressure for a slanted wall with a flat surface on top. In order to complete the theory of Coulomb (1776)[2], it is also necessary to derive the solution for a sloped backfill on top of the wall. Also, this is necessary for implementing the dynamic pressure on the wall based on Mononobe-Okabe's (1929 & 1924)[8,11] method. The Coulomb static and dynamic pressure for cohesive soil on a slanted wall with a sloped backfill is the subject addressed in this paper. The active and passive pressures are derived and compared with recent methods.

In the past, before the computer age, cumbersome analytical solutions were not preferred and graphical solutions were used. These solutions are such as the Culmann's (1866)[3] graphical method, and the Mohr (1871)[7] diagram for Rankine's (1857)[14] method. However, in the present time, cumbersome analytical solutions, such as in closed form solutions, are not a problem to implement on a computer and are preferred. Thus, errors can be avoided. In this paper the equations are cumbersome and long and contain as many

If the wall height is H then the forces for the height h below h_c are to be considered. The total weight W_T can be written as

$$W_T = \frac{\gamma z L}{2} \cos \alpha + q \left[\frac{h_c \sin \xi \cos \beta + L \cos \alpha \cos \beta}{\cos(\xi - \beta)} \right] + \gamma h_c \left[\frac{h_c \sin \xi \cos \beta + 2L \cos \alpha \cos \beta}{2 \cos(\xi - \beta)} \right] \dots (1)$$

where

$$L = \frac{z}{\sin \alpha + \cos \alpha \tan(\xi - \beta)}, \quad z = \frac{h}{\cos \xi}, \quad \text{and} \quad h = H - \frac{\cos \xi \cos \beta}{\cos(\xi - \beta)} h_c \dots (2)$$

Summing the forces in the x and z direction yields

$$E_{ax} = W_T \sin \xi + Q \sin(\alpha - \phi) - cL \cos \alpha \dots (3)$$

$$E_{az} = -c'z + W_T \cos \xi - Q \cos(\alpha - \phi) - cL \sin \alpha \dots (4)$$

where c' is the adhesion and it has the same sign as the friction angle δ on the wall.

Eliminating Q from Eq. 3 and 4, substituting $E_{az} = E_{ax} \tan \delta$, L and z from Eq. 2, and W_T from Eq. 1 yields

$$E_{ax} = \frac{\gamma h^2}{2} f(\alpha, \phi, \beta, \xi, \delta) + \gamma h g(\alpha, \phi, c, \beta, \xi, \delta, c') + t(\alpha, \phi, \beta, \xi) \dots (5)$$

where

$$f(\alpha, \phi, \beta, \xi, \delta) = \frac{\sin \xi + \cos \xi \tan(\alpha - \phi)}{[1 + \tan \delta \tan(\alpha - \phi)][\tan \alpha + \tan(\xi - \beta)] \cos^2 \xi} \dots (6)$$

$$g(\alpha, \phi, c, \beta, \xi, \delta, c') = \frac{[\sin \xi + \cos \xi \tan(\alpha - \phi)] \cos \beta}{[1 + \tan \delta \tan(\alpha - \phi)][\tan \alpha + \tan(\xi - \beta)] \cos(\xi - \beta) \cos \xi} \left[\frac{q}{\gamma} + h_c \right] - \frac{(c/\gamma)[\tan \alpha \tan(\alpha - \phi) + 1] + (c'/\gamma) \tan(\alpha - \phi)[\tan \alpha + \tan(\xi - \beta)]}{[1 + \tan \delta \tan(\alpha - \phi)][\tan \alpha + \tan(\xi - \beta)] \cos \xi} \dots (7)$$

$$t(\alpha, \phi, \beta, \xi) = \frac{[\sin \xi + \cos \xi \tan(\alpha - \phi)] \cos \beta \sin \xi}{[1 + \tan \delta \tan(\alpha - \phi)] \cos(\xi - \beta)} \left[\frac{q}{\gamma} + \frac{h_c}{2} \right] h_c \dots (8)$$

The total vertical force is $\bar{E}_{az} = E_{az} + c'z$ where $E_{az} = E_{ax} \tan \delta$, and the resultant force is

$E_a = \sqrt{E_{ax}^2 + \bar{E}_{az}^2}$. To maximize E_a it can be seen that E_{ax} can be maximized instead.

Rewriting Eq. 5 as

$$E_{ax} = \left(\frac{\gamma h^2}{2} \right) \left(\frac{l \tan^2 \alpha + m \tan \alpha + n}{u \tan^2 \alpha + v \tan \alpha + w} \right) \dots\dots\dots (9)$$

where

$$A = \frac{1}{\cos^2 \xi} + \left(\frac{2 \cos \beta}{\cos(\xi - \beta) \cos \xi} \right) \left(\frac{q}{\gamma h} + \frac{h_c}{h} \right) \dots\dots\dots (10)$$

$$B = \left(\frac{\sin \xi \cos \beta}{\cos(\xi - \beta)} \right) \left(\frac{h_c}{h} \right) \left(\frac{2q}{\gamma h} + \frac{h_c}{h} \right) \dots\dots\dots (11)$$

$$l = \frac{B \cos(\xi - \phi)}{\cos \phi} - \frac{2c}{\gamma h \cos \xi} - \frac{2c'}{\gamma h \cos \xi} \dots\dots\dots (12)$$

$$m = \frac{A \cos(\xi - \phi)}{\cos \phi} - \frac{2c' [\tan(\xi - \beta) - \tan \phi]}{\gamma h \cos \xi} + \frac{B \sin(2\xi - \beta - \phi)}{\cos \phi \cos(\xi - \beta)} \dots\dots\dots (13)$$

$$n = \frac{[A + B \tan(\xi - \beta)] \sin(\xi - \phi)}{\cos \phi} - \frac{2c}{\gamma h \cos \xi} + \frac{2c' \tan \phi \tan(\xi - \beta)}{\gamma h \cos \xi} \dots\dots\dots (14)$$

$$u = \tan \phi + \tan \delta \dots\dots\dots (15)$$

$$v = (\tan \phi + \tan \delta) \tan(\xi - \beta) + 1 - \tan \phi \tan \delta \dots\dots\dots (16)$$

$$w = (1 - \tan \phi \tan \delta) \tan(\xi - \beta) \dots\dots\dots (17)$$

Maximizing E_{ax} with respect to α yields $\frac{\partial E_{ax}}{\partial \alpha} = \frac{\partial(\tan \alpha)}{\partial \alpha} \frac{\partial E_{ax}}{\partial(\tan \alpha)} = 0$. Thus, $\tan \alpha$ can be

extracted from Eq. 9 as

$$\tan \alpha = -a \pm \sqrt{a^2 - b} \dots\dots\dots (18)$$

where

$$a = \frac{lw - nu}{lv - mu}, \text{ and } b = \frac{mw - nv}{lv - mu} \dots\dots\dots (19)$$

Therefore, evaluate l, m, n, u, v and w from Eq. 12 to 17 and substitute in Eq. 19 and find $\tan \alpha$ from Eq. 18. Substitute $\tan \alpha$ in Eq. 9 to find E_{ax} **maximum** or evaluate α and substitute in Eq. 5 to find E_{ax} **maximum**. Hence, the Coulomb active condition is obtained.

b) Passive Condition

To find the passive pressure E_{px} : set $h_c = 0$, replace ϕ by $-\phi$, c by $-c$, δ by $-\delta$, and c' by $-c'$ in Eq. 12 to 17 and evaluate $\tan \alpha$ and α from Eq. 18. Substitute $\tan \alpha$ in Eq. 9 and obtain E_{px} **minimum** the passive force normal to the wall. Alternatively, substitute α in the following equation to obtain E_{px} **to find the minimum**:

$$E_{px} = \frac{\gamma h^2}{2} f(\alpha, -\phi, \beta, \xi, -\delta) + \gamma h g(\alpha, -\phi, -c, \beta, \xi, -\delta, -c') \dots\dots\dots (20)$$

The total vertical force \bar{E}_{pz} , and the resultant E_p can be obtained from:

$$\bar{E}_{pz} = E_{px} \tan \delta + c' z, \text{ and } E_p = \sqrt{\bar{E}_{pz}^2 + E_{px}^2} \dots\dots\dots (21)$$

Note: δ and c' are considered positive when the tangential force is downward on the wall. This is consistent with standard practice for the passive condition. On the other hand, in the active condition, δ and c' are considered positive when the tangential force is upward on the wall.

c) Pressure Diagram

The active pressure distribution, σ_{ax} , normal to the wall can be found by taking

$$\sigma_{ax} = \frac{\partial E_{ax}}{\partial z} = \cos \xi \frac{\partial E_{ax}}{\partial h} . \text{ Differentiating Eq. 5 yields}$$

$$\sigma_{ax} = (\gamma h \cos \xi) f(\) + (\gamma \cos \xi) g(\) + \cos \xi \left[\frac{\gamma h^2}{2} \frac{\partial f(\)}{\partial h} + \gamma h \frac{\partial g(\)}{\partial h} + \frac{\partial (\)}{\partial h} \right] \dots\dots\dots (22)$$

The right hand term in the brackets in Eq. 22 can be written as $\frac{\partial \alpha}{\partial h} \frac{\partial E_{ax}}{\partial \alpha}$, which is zero since α is from Eq. 18. Thus, the active pressure normal to the wall becomes:

$$\sigma_{ax} = (\gamma h \cos \xi) f(\alpha, \phi, \beta, \xi, \delta) + (\gamma \cos \xi) g(\alpha, \phi, c, \beta, \xi, \delta, c') \dots\dots\dots (23)$$

The upward tangential shear on the wall becomes:

$$\tau_{axz} = \sigma_{ax} \tan \delta + c' \dots\dots\dots (24)$$

Similarly, the passive pressure, σ_{px} , normal to the wall becomes

$$\sigma_{px} = (\gamma h \cos \xi) f(\alpha, -\phi, \beta, \xi, -\delta) + (\gamma \cos \xi) g(\alpha, -\phi, -c, \beta, \xi, -\delta, -c') \dots\dots\dots (25)$$

where $h_c = 0$ in the $g()$ function. The downward tangential shear on the wall becomes:

$$\tau_{pxz} = \sigma_{px} \tan \delta + c' \dots\dots\dots (26)$$

d) Example (1)

(See example by Prabhakara (1965)[12]) Determine the active force against a vertical wall 12m (39.37ft) in height with the following data available:

$$\phi = 30 \text{ degrees} \quad \delta = +20 \text{ degrees} \quad c = c' = 1250 \text{ kg/m}^2 \text{ (255.58 lb/ft}^2 \text{)}$$

$$\xi = \beta = 0 \quad q = 0 \quad \gamma = 1870 \text{ kg/m}^3 \text{ (116.66 lb/ft}^3 \text{)}$$

$$h_c = \frac{4c}{\gamma} \tan(45 + \phi / 2) = 4.63 \text{ m (15.19 ft)}, \quad h = H - h_c = 12 - 4.63 = 7.37 \text{ m (24.18 ft)}$$

Substituting in Eq. 10 through 19 yields ($A = 2.257, B = 0, l = -0.363, m = 2.362, n = -1.484, u = 0.941, v = 0.790, w = 0, a = -0.557, b = -0.467$), $\tan \alpha = 1.438$, and $\alpha = 55.19$

degrees. Substituting $\tan \alpha = 1.438$ in Eq. 9 yields $E_{ax} / (0.5\gamma h^2) = 0.3768$. Thus,

$$E_{ax} = 19,129 \text{ kg / m (12.84 kips / ft)}, \quad E_{az} = E_{ax} \tan \delta = 6,962 \text{ kg / m (4.67 kips / ft)},$$

and $\sqrt{E_{ax}^2 + E_{az}^2} = 20,356 \text{ kg / m (13.67 kips / ft)}$. This number matches Prabhakara

within 1%, a slide rule error. However, $\bar{E}_{za} = E_{az} + c'h = 16,173 \text{ kg / m (10.68 kips / ft)}$,

and the actual resultant is $E_a = \sqrt{E_{ax}^2 + \bar{E}_{za}^2} = 25,050 \text{ kg / m (16.82 kips / ft)}$.

e) **Critical Height h_c**

If assuming $\xi = 0$, $q = 0$, $\delta = 0$, and $c' = 0$, then $h_c = (4c / \gamma) \tan(\pi / 4 + \phi / 2)$ can be used for a wall with a flat surface on top, and possibly for a semi-infinite soil with a sloped surface on top with an angle β , see Terzaghi (1943)[20]. However, for other conditions, h_c will vary with many parameters besides c , γ , and ϕ . Additionally, based on an existing crack intersecting the slip surface, Terzaghi (1943)[20] showed that the critical height can be as low as $h_c = (2.67c / \gamma) \tan(\pi / 4 + \phi / 2)$. To find the exact h_c : set $h_c = 0$, $\delta = 0$, and $c' = 0$ in all the equations for the active condition, then solve for h that makes $E_{ax} = 0$ in Eq. 5 or Eq. 9. This can be done by Newton Raphson's iteration, the secant method, which can be found in any numerical analysis textbook. Then $h_c = h^* \cos(\xi - \beta) / (\cos \beta \cos \xi)$ where h^* is the root of the equation $E_{ax} = 0$. Note: there exists a maximum of two roots. One of the roots is $h^* = 0$ and it is not desirable. The initial h value in the iteration should be selected large enough to extract the desirable second root. Consequently, the theoretical h_c can be extracted. To obtain Terzaghi's reduction simply reduce h_c by 2/3. If σ_{ax} in Eq. 23 is greater than zero at $h = 0$, then the iteration will converge to $h^* = 0$ and h_c cannot be found. This situation will occur since $\sigma_{ax} (@h = 0) = \gamma g(\alpha, \phi, c, \beta, \xi, 0, 0)$ and it can take a positive value for some surcharge q .

f) **Example (2)**

Determine the active force against a slanted wall $\xi = +5$ degrees, 10 m (32.81 ft) high, with a sloped backfill $\beta = 20$ degrees, for the available data

$$\phi = 30 \text{ degrees} \quad q = 1140 \text{ kg/m}^2 (233.09 \text{ lb/ft}^2) \quad c = 1250 \text{ kg/m}^2 (255.58 \text{ lb/ft}^2)$$

$$\delta = 20 \text{ degrees} \quad c' = 1000 \text{ kg/m}^2 (204.5 \text{ lb/ft}^2) \quad \gamma = 1870 \text{ kg/m}^3 (116.66 \text{ lb/ft}^3)$$

Use theoretical h_c and compare with using $h_c = (4c / \gamma) \tan(45 + \phi / 2) = 4.63 \text{ m} (15.19 \text{ ft})$.

$$\text{case (i): } h_c = (4c / \gamma) \tan(45 + \phi / 2) = 4.63 \text{ m} (15.19 \text{ ft}):$$

Thus, $h = 10 - 4.63(.969) = 5.512 \text{ m} (18.08 \text{ ft})$. Substituting in Eq. 10 through 19 yields

$$(A = 2.865, B = 0.076, l = -0.359, m = 3.105, n = -1.662, u = 0.845, v = 0.619,$$

$$w = -0.226, a = -0.522, b = -0.114), \tan \alpha = 1.144, \text{ and } \alpha = 48.84 \text{ degrees. Substituting}$$

$$\tan \alpha \text{ in Eq. 9 yields } E_{ax} / (0.5\gamma h^2) = 0.8943. \text{ Thus, } E_{ax} = 25,403 \text{ kg / m} (17.06 \text{ kips / ft}),$$

$$\bar{E}_{za} = E_{ax} \tan \delta + c' h = 12,339 \text{ kg / m} (8.29 \text{ kips / ft}), \text{ and the resultant is}$$

$$E_a = \sqrt{E_{ax}^2 + \bar{E}_{za}^2} = 28,241 \text{ kg / m} (18.96 \text{ kips / ft}).$$

case (ii) Theoretical h_c :

Set $h_c = 0$, $\delta = 0$, and $c' = 0$ in all the equations and solve for $h = h^* = 2.8139 \text{ m} (9.232 \text{ ft})$

that makes $E_{ax} = 0$. Thus, $h_c = 2.903 \text{ m} (9.525 \text{ ft})$ with $(A = 1.431, B = 0, l = -0.477, m =$

$$1.497, n = -1.175, u = 0.577, v = 0.845, w = -0.268, a = -0.636, b = -0.467, \tan \alpha = 1.57,$$

and $\alpha = 57.5 \text{ degrees})$ making $E_{ax} = 0$. By using $h_c = 2.903 \text{ m} (9.525 \text{ ft})$, and

$$h = 10 - 2.903(.969) = 7.186 \text{ m} (23.58 \text{ ft}), \text{ substituting in Eq. 10 through 19 yields } (A =$$

$$1.962, B = 0.02, l = -0.316, m = 2.165, n = -1.165, u = 0.845, v = 0.619,$$

$$w = -0.226, a = -0.522, b = -0.114), \tan \alpha = 1.143, \text{ and } \alpha = 48.81 \text{ degrees. Substituting}$$

$$\tan \alpha \text{ in Eq. 9 yields } E_{ax} / (0.5\gamma h^2) = 0.5660. \text{ Thus, } E_{ax} = 27,331 \text{ kg / m} (18.35 \text{ kips / ft}),$$

$\bar{E}_{za} = E_{ax} \tan \delta + c'h = 14,537 \text{ kg / m (9.76 kips / ft)}$, and the resultant is

$$E_a = \sqrt{E_{ax}^2 + \bar{E}_{az}^2} = 30,957 \text{ kg / m (20.79 kips / ft)}.$$

Hence, the increase in the resultant due to the difference in the critical height h_c in case (i) and (ii) is 9.62% which is considerable due to the surcharge.

g) Comparison of Coulomb Equations with Rankine Equations

Historically, Rankine's (1857)[14] solution for cohesion is popular since it is very easy to do a graphical method on a Mohr diagram (see Terzaghi (1943)[20] and Kézdi in Winterkorn and Hsai-Yang (1975)[22]). On the other hand, Coulomb method required several trial surfaces before reaching the optimal forces. For a semi-infinite mass with a plane surface at an angle β to the horizontal and with vertical wall ($\xi = 0$), [similarly](#) the Rankine stress can be written as [\(formula revised\)](#)

$$\sigma_{ax} \text{ (Rankine)} = \cos^2 \beta \left[-1 + 2 \frac{\cos^2 \beta}{\cos^2 \phi} + 2 \left(\frac{c}{\gamma z} \right) \tan \phi - 2\gamma \sqrt{a_0 + b_0 + c_0} \right] \gamma z \dots\dots\dots (27)$$

where

$$a_0 = \left(\frac{c}{z\gamma} \right)^2 \frac{1}{\cos^2 \phi}, \quad b_0 = \frac{2c}{z\gamma} \tan \phi \left(\frac{\cos \beta}{\cos \phi} \right)^2, \quad \text{and} \quad c_0 = \left(\frac{\cos \beta}{\cos \phi} \right)^4 - \left(\frac{\cos \beta}{\cos \phi} \right)^2$$

When allowing tension ($h_c = 0$), the active resultant force can be expressed as

$$E_a = \int_0^h \sigma_{ax} dz \text{ and has a directional angle } \beta. \text{ Note: in Rankine method the friction and the}$$

adhesion on the wall do not enter the equation (Eq. 27). Thus, the Rankine method is

considered an approximation. One major difference between the Rankine and the Coulomb method for cohesion is that with the Rankine method the directional angle of the resultant is constant and is equal to β . On the other hand, with the Coulomb method the directional angle varies with depth when there is adhesion. The shear due to the adhesion on the wall increases with depth but the directional angle $[\tan \delta + (c' / \gamma z)] / (E_{ax} / \gamma z^2)$ decreases. At $z \rightarrow \infty$ the directional angle becomes δ . Since the adhesion and the friction on the wall are essential parameters, then it is clear that the Coulomb equation is more accurate than the Rankine equation. The results show that the Rankine equation seems to be **not** conservative. Even when setting $c' = 0$, one finds the equations do not match. For example if set $c' = 0$, $\delta = \beta = \phi = 30$ degrees, $h_c = q = 0$, and $c / (\gamma z) = 0.1$, then $E_a / (0.5 \gamma h^2) = 0.3317$ for Coulomb and $E_a / (0.5 \gamma h^2) = 0.2983$ for Rankine, a difference of **11.2 %**. Note: in the case of granular material the equations match when $\delta = \beta$ with $\xi = 0$. Also, in the case of granular material the Rankine equation has been used as an approximation (see Das (1994)[4]).

h) Comparison of Coulomb Passive Pressure with Log-Spiral Method of Slices

Shields and Tolunay (1973)[19] did a modified Terzaghi (1943)[20] analysis for passive pressure in granular material on a wall with positive friction. In their solution they used the method of slices and assumed the vertical shear to be zero on each slice except for the first slice next to the wall. The slip surface they used is a logarithmic spiral and their results were close to experimental findings. Basudhar and Madhav (1980)[1] repeated the analysis and included cohesion and pore pressure. In their analysis they did not use the

same initial angle² α_w at the wall between the logarithmic spiral and the horizontal.

Instead, they optimized the function with respect to the center of the logarithmic spiral. In many ways the optimization could also have been done with respect to α_w instead of the center of the logarithmic spiral. Rewriting the logarithmic spiral equations to include the surcharge q with $h_c = 0$, the slice horizontal force can be found from Eq. 5, yielding

$$dE_{px} = (\gamma z dz) f(\alpha, -\phi, 0, 0, 0) + (\gamma dz) g(\alpha, -\phi, -c, 0, 0, 0) \dots\dots\dots (28)$$

where

$$z = z_0 + r_0 \cos(\alpha + \phi) e^{\tan \phi (\alpha - \alpha_w)} \dots\dots\dots (29)$$

$$dz = r_0 d\alpha \sin \alpha \sec \phi e^{\tan \phi (\alpha - \alpha_w)} \dots\dots\dots (30)$$

$$z_0 = -r_0 \tan \psi \sin(\phi + \alpha_w) \dots\dots\dots (31)$$

$$r_0 = h \cos \psi \sec(\psi + \phi + \alpha_w) \dots\dots\dots (32)$$

$$\psi = \pi / 4 - \phi / 2 \dots\dots\dots (33)$$

$$f(\alpha, -\phi, 0, 0, 0) = \tan(\alpha + \phi) \cot \alpha \dots\dots\dots (34)$$

$$g(\alpha, -\phi, -c, 0, 0, 0) = (q / \gamma) \tan(\alpha + \phi) \cot \alpha + (c / \gamma) [\tan \alpha \tan(\alpha + \phi) + 1] \cot \alpha \dots\dots\dots (35)$$

and α is the slice wedge angle with the horizontal. Summing all the horizontal forces of all the slices except for the slice next to the wall, yields

$$\int dE_{px} = \int \left[\gamma z \frac{dz}{d\alpha} f(\alpha) + \gamma \frac{dz}{d\alpha} g(\alpha) \right] d\alpha = \gamma \frac{r_0^2}{2} \sin^2(\alpha + \phi) e^{2 \tan \phi (\alpha - \alpha_w)} - \gamma r_0 \left[z_0 + \frac{q}{\gamma} \right] \cos(\alpha + \phi) e^{\tan \phi (\alpha - \alpha_w)} + \gamma r_0 \left[\left(z_0 + \frac{q}{\gamma} \right) \tan \phi + \frac{c}{\gamma} \right] \int \sec(\alpha + \phi) e^{\tan \phi (\alpha - \alpha_w)} d\alpha \dots\dots\dots (36)$$

² In a later article by the author 2007 titled “Kp for a Wall with Friction with Exact Slip Surface” the initial angle α_w by Shields and Tolunay (1973)[19] is correct.

where the integral $\int dE_{px}$ in Eq. 36 needs to be evaluated from α_w to ψ . Thus, the passive force can be expressed as

$$E_{px} = \frac{P_R + \int_{\alpha_w}^{\psi} dE_{px} + c' h \tan(\alpha_w + \phi)}{1 - \tan \delta \tan(\alpha_w + \phi)} \dots\dots\dots (37)$$

where

$$P_R = \left[\frac{\gamma}{2} h_0^2 + q h_0 \right] \tan^2(\pi/4 + \phi/2) + 2c h_0 \tan(\pi/4 + \phi/2) \dots\dots\dots (38)$$

and $h_0 = z_0 + r_0 \sin \psi e^{\tan \phi(\psi - \alpha_w)}$. Hence, for a given h pick α_w and find r_0 and z_0 from Eq. 32 and 31, evaluate the integral $\int dE_{px}$ from Eq. 36 from $\alpha = \alpha_w$ to $\alpha = \psi$ and integrate numerically the last term in the equation, then evaluate P_R from Eq. 38 and substitute in Eq. 37 to evaluate E_{px} for a given positive δ and c' . Repeat the process with different α_w until E_{px} minimum is found.

For granular soil with $q = c = c' = 0$ the results match Basudhar and Madhav (1980)[1].

Also, the results match Shields and Tolunay (1973)[19] if

$$\alpha_w = 0.5 \left\{ \arccos[\cos(\phi - \delta) - \sin(\phi - \delta) \cot \phi] - \phi - \delta \right\} \text{ where } \delta \text{ takes a positive value.}$$

Comparing Eq. 37 with Coulomb Eq. 20 with $\xi = \beta = 0$, yields the curves in Fig. 2 where

$2E_{px} / (\gamma h^2)$ is plotted against δ for $\rho = c' / (\gamma h) = c / (\gamma h) = 0, 0.1, \text{ and } 0.2, \phi = 30$

degrees, and $q = 0$. Note: for $\delta > \phi/3$ the difference is very large. However, for $\delta \leq \phi/3$

the Coulomb method and the logarithmic spiral method of slices are close, within 11% at maximum point. This is a reasonable cut-off point for the Coulomb equation. Terzaghi (1943)[20] recommended $\delta \leq \phi / 3$ be used for computing the passive pressure by means of Coulomb's equation for granular soil. This is also the author's recommendation for cohesive soil. This is necessary since both methods have been traditionally used.

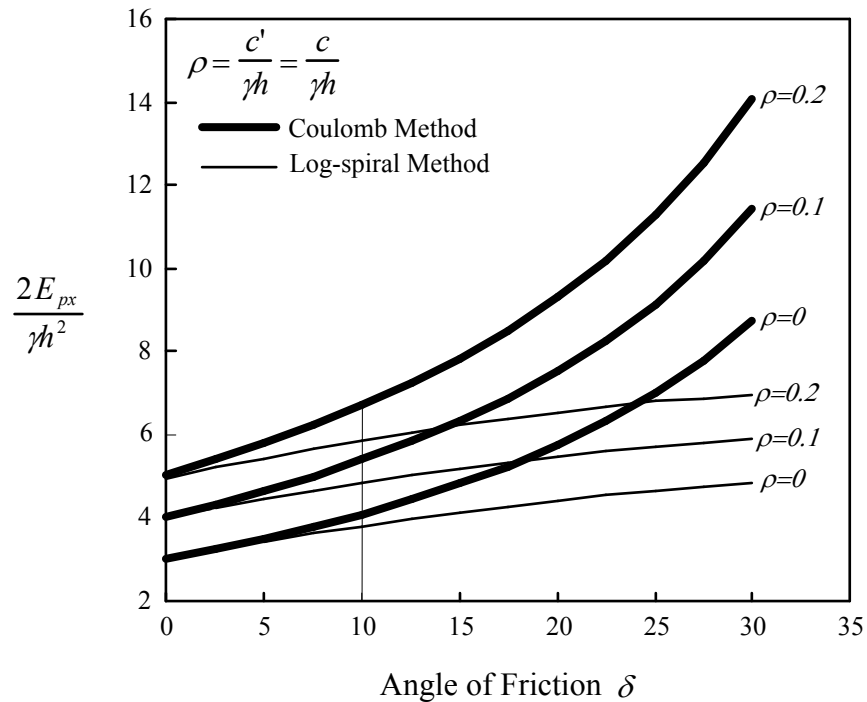


FIG. 2 - Passive Pressure Coefficient with Cohesion

CASE II: DYNAMIC CONDITION

Since Mononobe and Okabe (1929 & 1924)[8,11] developed a method, by modifying Coulomb's solution, to evaluate dynamic earth pressures against retaining structures, a number of studies have been performed on this subject in granular soil, but not many in cohesive soil. Prakash and Saran (1966)[13] derived an equation for dynamic active cohesive soil pressure against retaining structure on the assumptions mostly employed by

Mononobe-Okabe. They adapted the pseudo-static approach in considering the dynamic effect of the backfill soil where they included the contributions of soil cohesion and uniform backfill surcharge to the dynamic lateral pressure. An allowance for tension cracks due to cohesion was also made. Since the Coulomb equation Eq. 5 is now complete and has the effect of slop backfill (β angle), the full dynamic range can be employed instead of the pseudo-static approach.

a) **Active Condition**

Following Mononobe and Okabe (1929 & 1924)[8,11], replace H by $H \sec \xi \cos(\xi + \theta)$, h by $H \sec \xi \cos(\xi + \theta) - h_c \sec(\xi - \beta) \cos(\xi + \theta) \cos(\beta + \theta)$, γ by $\gamma(1 - k_v) \sec \theta$, ξ by $\xi + \theta$, and β by $\beta + \theta$ in Eq. 10 through 17, where $\theta = \arctan[k_h / (1 - k_v)]$, k_h and k_v are the horizontal and vertical acceleration coefficients. Thus, by substituting in Eq. 18 to find $\tan \alpha$, then in Eq. 9, E_{ax} can be found. This simple procedure yields the seismic resultant active force E_{aE} and its directional angle δ_E to be

$$E_{aE} = \sqrt{E_{ax}^2 + (E_{ax} \tan \delta + c'z)^2} \dots\dots\dots (39)$$

$$\delta_E = \frac{E_{ax} \tan \delta + c'z}{E_{ax}} \dots\dots\dots (40)$$

Often the interest is in the horizontal component of the resultant force. The horizontal component can be written as:

$$E_{aE,h} = E_{aE} \cos(\delta_E + \xi) \dots\dots\dots (41)$$

Note: h_c needs to be evaluated independently as described in section e) in the CASE I-Static Condition. If the soil can take tension then $h_c = 0$.

b) Passive Condition

Following Mononobe and Okabe (1929 & 1924)[8,11], replace h by $h \sec \xi \cos(\xi + \theta)$, γ by $\gamma(1 - k_v) \sec \theta$, ξ by $\xi - \theta$, β by $\beta - \theta$, ϕ by $-\phi$, δ by $-\delta$, c' by $-c'$, and set $h_c = 0$ in Eq. 10 through 17. By substituting in Eq. 18 to find $\tan \alpha$, then in Eq. 9, E_{px} can be found. This simple procedure yields the seismic resultant passive force E_{pE} and its directional angle δ_E to be

$$E_{pE} = \sqrt{E_{px}^2 + (E_{px} \tan \delta + c'z)^2} \dots\dots\dots (42)$$

$$\delta_E = \frac{E_{px} \tan \delta + c'z}{E_{px}} \dots\dots\dots (43)$$

The horizontal component can be written as:

$$E_{pE,h} = E_{pE} \cos(\delta_E + \xi) \dots\dots\dots (44)$$

Note: the solution is valid only for $\delta \leq \phi / 3$ as was pointed out in the static case.

c) Comparison with Recent Method

Richards and Shi (1994)[18] derived an elasto-plastic free field solution for earthquakes acting on cohesive soil which they applied the solution directly to retaining structures. For granular soil prior work in elasto-plastic was performed by Richards et al. (1990)[17].

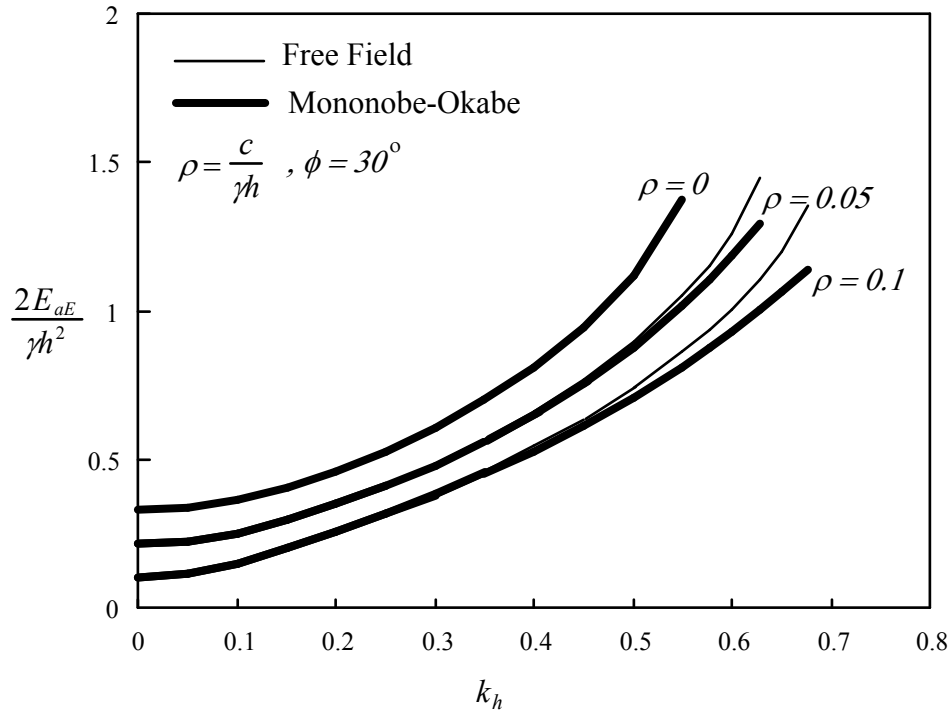
One major difference between applying their method and the Mononobe-Okabe method proposed in this paper (Eq. 39 and 42) is when $\theta = 0$, the static condition, in their solution the stresses are assumed linear and the shear is zero at the wall. This assumption was necessary in their solution using the elasto-plastic fluidization of soil. However, for a wall to develop no shear at $\theta = 0$ is not likely and is apparent in the Coulomb method.

Furthermore, the pressure can be nonlinear per Eq. 23 and 25. This makes the Mononobe-Okabe method proposed in this paper more applicable. However, the simple free-field solution, will give the correct stresses on a retaining wall if it deforms exactly as dictated by the free-field thereby maintaining the correct interface boundary condition. In order to compare Eq. 39 with Richards and Shi (1994)[18] equations, the friction and the adhesion on the wall must correspond to their assumption. For granular soil they showed that $\tan \delta$ must equal $\tan \theta / K_{AE}$ in order to match Mononobe-Okabe method, where K_{AE} is from their paper. Similarly, for cohesive soil it is necessary to set the adhesion $c' = 0$, to allow δ to be greater than ϕ , and use

$$\tan \delta = \frac{T_{AE}}{N_{AE}} \dots\dots\dots (45)$$

where T_{AE} and N_{AE} are from Richards and Shi's paper. Setting, $k_v = 0$, $c' = 0$, $q = 0$, $\phi = 30$ degrees, $h_c = 0$, and $\xi = \beta = 0$ in all the equations that lead to Eq. 39, and plotting the normalized seismic resultant active force $2E_{ae} / (\gamma h^2)$ versus k_h for both methods using $\rho = c/\gamma h = 0, 0.05$, and 0.1 yields the curves in Fig. 3. The results show the free-field

solution is more conservative than the Mononobe-Okabe solution: about 19% increase at the worst point on Fig. 3.



For the passive pressure, replace T_{AE} and N_{AE} in Eq. 45 by T_{PE} and N_{PE} from Richards and Shi's paper. Setting, $k_v = 0, c' = 0, q = 0, \phi = 30$ degrees, $\xi = \beta = 0$, and all the passive and

FIG. 3 - Comparison of Free Field and Mononobe-Okabe's Method for Active Thrust
for Case with Tension Allowed ($h_c = 0$)

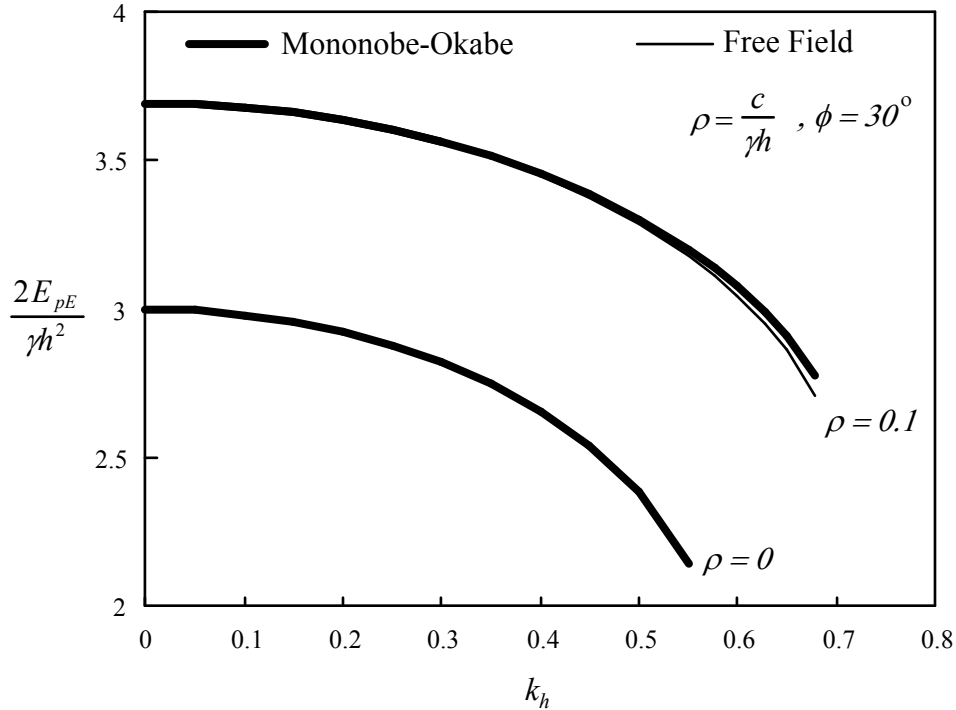


FIG. 4 - Comparison of Free Field and Mononobe-Okabe's Method for Passive Thrust

seismic requirements in all the equations that lead to Eq. 42, and plotting the normalized seismic resultant passive force $2E_{pE} / (\gamma h^2)$ versus k_h for both methods using $\rho = c/\gamma h = 0$, and 0.1 yields the curves in Fig. 4. The results show the free-field solution is slightly more conservative than the Mononobe-Okabe solution: about 3% decrease at the worst point on Fig. 4.

d) Design Criteria

Even in moderate earthquakes, gravity walls without lateral bracing slide at their base (Richards and Elms (1979)[16]). For cohesionless soil the total thrust for different wall movement has been traditionally calculated using Mononobe-Okabe's equation. Also, the total thrust is almost the same as that calculated by free-field analysis (Richards

(1991)[15]) and can also be used for $\beta = \xi = 0$. Similarly, for cohesive soil, the thrust calculation can be used from the Mononobe-Okabe Eq. 39 as well from the free-field equation of Richards and Shi for $\beta = \xi = 0$. Thus, for sliding failure, the straightforward method presented by Richards and Elms (1979) [16] for cohesionless soil and Richards and Shi (1994)[18] for cohesive soil can be extended for limit analysis and design with cohesive soil that includes β and ξ slope angle configurations. The extended analysis yields

$$W_w = \frac{E_{aE} [\cos(\delta_E + \xi) - \tan \phi_b \sin(\delta_E + \xi)] - c'' B_w}{(1 - k_v)(\tan \phi_b - \tan \theta)} \dots\dots\dots (46)$$

where W_w is the self-weight of the retaining wall, E_{aE} and δ_E are from Eq. 39 and 40, ϕ_b is the friction angle between the soil and the bottom of the wall, B_w is the base dimension of the wall, and c'' is the adhesion on the base. When using Eq. 46 to map the ratio of the W_w over the static weight versus k_h (for $k_v = 0$), the results show that the seismic magnification for cohesive soil is even more dramatic than sand. This has been pointed out by Richards and Shi (1994)[18]. Thus, for a given safety factor or weight to static weight ratio the critical acceleration value k_h^* can be determined for a particular wall using Eq. 46. Consequently, the seismic displacement for design can be obtained and controlled by using Newmark's (1965) [10] sliding-block approach developed by Richards and Elms (1979) [16] for walls. The incremental accumulation of displacement can also be calculated by a more sophisticated method (Nadim and Whitman (1983) [9]) that is less conservative. Conversely, the wall can be designed to limit seismic

deformation to a tolerable value for the earthquake intensity specified by (Elms & Richards (1979) [5]; Whitman and Liao (1985) [21]) as recommended by AASHTO ("Foundation" (1992) [6]).

Summary and Conclusions

The static Coulomb equations for a slanted wall with sloped backfill in cohesive soil are finally completed in this paper. Furthermore, the solution is extended to derive the dynamic earth pressure for cohesive soil per Mononobe-Okabe. The static active Coulomb equation is obtained and is expected to give realistic forces and pressure on a retaining wall in cohesive soil. Also, the active solution is compared with the Rankine method. The results show that the Rankine solution is **not** conservative and it is considered an approximation. As expected, the Coulomb passive equation is not adequate for $\delta > \phi/3$ and the logarithmic-spiral method of slices is recommended as it was the case for cohesionless soil. The earthquake solution is obtained and compared with the free-field solution. In order to compare, the friction and the adhesion on the wall was made to correspond to the free-field assumption. Noting that the proposed solution in this paper is of more general application than the free-field solution. The results show that the free-field solution is slightly more conservative than the Mononobe-Okabe equations presented in the paper. The proposed general solutions are consistent with the classical methods and complete the Coulomb equations of earth pressures.

Acknowledgments

The writer is deeply appreciative to his wife Bernice J.F. Chouery for the love and patience in giving valuable family support to do this manuscript. Also, he is thankful to the assistance provided by Shirley A. Egerdahl in proofreading this manuscript.

Appendix I.-References

1. Basudhar, P. K., and Madhav, M. R. (1980). "Simplified Passive Earth Pressure Analysis," *Journal of the Geotechnical Engineering Division, ASCE*, Vol. 106, No. GT4, pp. 470-474.
2. Coulomb, Charles Augustin (1776). "Essai sur une application des règles de maximis et minimis à quelques problèmes de statique relatifs à l'architecture," *Mem. Div. Savants, Acad. Sci., Paris*, Vol. 7.
3. Culmann, C. (1866), *Graphische Statik*, Zürich.
4. Das, B. M. (1994). Principles of Geotechnical Engineering, PWS Publishing Company, Boston, Massachusetts, Chapter 10, pp. 421-423.
5. Elms, D. G., and Richards, R. (1979). "Seismic Design of Gravity Retaining Walls," *Bull. of the New Zealand Nat. Soc. for Earthquake Engrg.*, 12(2), pp. 114-121.

6. "Foundation and Abutment Design Requirements," (1992). *Division I-A – seismic design commentary, sec. 6*. American Association of State Highway and Transportation Officials (AASHTO), pp. 393-400.
7. Mohr, O. (1871). "Beiträge zur Theorie des Erddruckes," *Z. Arch. u. Ing. Ver. Hannover*, Vol. 17 (1871), p. 344, and Vol. 18 (1872), pp. 67, 245.
8. Mononobe, N. (1929). "Earthquake-Proof Construction of Masonry Dams," *Proceedings of the world Engineering Conference*, Vol. 9, p. 275.
9. Nadim, F., and Whitman, R. V. (1983). "Seismically Induced Movement of Retaining Walls," *J. Geotech. Engrg.*, ASCE, 109(7), pp. 915-931.
10. Newmark, N. M. (1965). "Effects of Earthquakes on Dams and Embankments," *Géotechnique*, London, England, 15(2), pp. 139-160.
11. Okabe, S. (1924). "General Theory of Earth Pressure," *Journal of Japanese Society of Civil Engineers*, Tokyo, Japan, Vol. 12, No. 1.
12. Prabhakara, K. S. (1965). "Analysis of Active Earth Pressure by Dimensionless Parameters," *Journal of India National Society of Soil Mechanics and Foundation Engineering*, April 1965, Vol. 4, No. 2, pp. 197-206.
13. Prakash, S., and Saran, S. (1966). "Static and Dynamic Earth Pressures Behind Retaining Walls," *Proc. Third Symposium on Earthquake Engrg.* Roorkee, India, pp. 277-288.
14. Rankine, W. J. M. (1857). "On the stability of loose earth," *Trans. Royal Soc.*, London, 147.

15. Richards, R. (1991). "Dynamic Earth Pressure and Seismic Design of Earth Retaining Structures," *Proc., 2nd Int. Conf. on Recent Adv. in Geotech. Earthquake Engrg. and Soil Dynamic, Vol. 3, General Rep. no. IV*, St. Louis, Mo., pp. 2033-2038.
16. Richards, R., and Elms, D. G. (1979). "Seismic Behavior of Gravity Retaining Walls," *Journal of the Geotechnical Engineering Division, ASCE*, Vol. 105, No. GT4, pp. 449-464.
17. Richards, R., Elms, D. G., and Budhu, M. (1990). "Dynamic Fluidization of Soils," *J. Geotech. Engrg.*, ASCE, 116(5), pp. 740-759.
18. Richards, R., and Shi, X. (1994). "Seismic Lateral Pressure in Soils with Cohesion," *J. Geotech. Engrg.*, ASCE, 120(7), pp. 1230-1251
19. Shields, D. H., and Tolunay, A. Z., (1973). "Passive Pressure Coefficients by Method of Slices," *Journal of the Soil Mechanics and Foundations Division, ASCE*, Vol. 99, No. SM12, Proc. Paper 10221, pp. 1043-1053.
20. Terzaghi, Karl (1943). *Theoretical Soil Mechanics*, Wiley and Sons, New York, pp. 39, pp. 152-155, pp. 38-41, pp. 113-117, and pp. 107.
21. Whitman, R. V., and Liao, S. (1985). "Seismic Design of Gravity Retaining Walls," *Misc. Paper GL-85-1*, U.S. Army Corp of Engineering, Vicksburg, Miss.
22. Winterkorn, H. F., and Hsai-Yang, F. (1975). *Foundation Engineering Handbook*, Van Nostrand Reinhold Co., New York, N. Y., Chapter 5, by Á. Kézdi, pp. 209-211, and pp. 200-203.

Appendix II.- Notation

The following symbols are used in this paper:

- α = wedge angle between a line parallel to the x -axis and the slip surface;
- β = slope angle of backfill between the top surface and the horizontal line;
- B_w = the base dimension of the wall;
- c = soil cohesion;
- c' = adhesion on the wall;
- c'' = adhesion between the wall base and soil;
- δ = friction angle between back face of wall and soil;
- δ_E = direction angle of seismic force of the wall;
- E_a = resultant active force on the wall;
- E_{aE} = seismic active resultant force;
- E_{ax} = active force normal to the wall;
- E_{az} = active force tangent to the wall;
- \bar{E}_{az} = active force tangent to the wall including wall adhesion;
- E_p = resultant passive force on the wall;
- E_{pE} = seismic passive resultant force;
- E_{px} = passive force normal to the wall;
- \bar{E}_{pz} = passive force tangent to the wall including wall adhesion;
- ϕ = angle of internal friction of soil;
- ϕ_b = friction angle between the soil and the bottom of the wall;
- h_c = critical height zone of tension cracks;

- q = surcharge load;
- σ_{ax} = active pressure normal to the wall;
- σ_{px} = passive pressure normal to the wall;
- τ_{axz} = active pressure tangent to the wall including wall adhesion;
- τ_{pxz} = passive pressure tangent to the wall including wall adhesion;
- W_w = the self weight of the retaining wall, and
- ξ = slanted angle between the vertical line and the wall.